Molecular Pharmacology Fast Forward. Published on April 13, 2009 as doi:10.1124/mol.109.055855
This article has not been copyedited and formatted. The final version may differ from this version.

MOL 55855

Potent Activity of Indolequinones against Human Pancreatic Cancer: Identification of Thioredoxin Reductase as a Potential Target

Chao Yan, Biehuoy Shieh, Philip Reigan, Zhiyong Zhang, Marie A. Colucci, Aurélie Chilloux, Jeffery J. Newsome, David Siegel, Dan Chan, Christopher J. Moody, and David Ross

Department of Pharmaceutical Sciences and Cancer Center, School of Pharmacy (C.Y., B.S., P.R., D.S., D.R.); Department of Medical Oncology, School of Medicine (Z.Z., D.C.), University of Colorado Denver, Denver, USA.

School of Chemistry, University of Nottingham, Nottingham NG7 2RD, United Kingdom (M.A.C., A.C., C.J.M.).

Department of Chemistry, University of Exeter, Exeter, EX4 4QD, United Kingdom (J.J.N).

Molecular Pharmacology Fast Forward. Published on April 13, 2009 as DOI: 10.1124/mol.109.055855
This article has not been copyedited and formatted. The final version may differ from this version.

MOL 55855

Running title: Indolequinone Antitumor Activity in Pancreatic Cancer

Corresponding Author: David Ross, Department of Pharmaceutical Sciences, School of Pharmacy, University of Colorado Denver, C-238, 12700 East 19th Avenue, Aurora, CO 80045, USA. Phone: 330-724-7265; Fax: 303-724-7266. Email: david.ross@ucdenver.edu

Number of text pages: 37

Number of tables: 2

Number of figures: 7

Number of references: 31

Number of words in Abstract: 243

Introduction: 334

Discussion: 1288

Abbreviations:

NQO1, NAD(P)H:quinone oxidoreductase 1

NQO2, NRH:quinone oxidoreductase 2

NRH, dihydronicotinamide riboside

MTT, 3-(4,5-Dimethylthiazol-2-yl)-2,5-diphenyltetrazolium bromide

Trx, thioredoxin

TrxR, Thioredoxin reductase

IQ, Indolequinone

BIAM, biotin-conjugated iodoacetamide

Molecular Pharmacology Fast Forward. Published on April 13, 2009 as DOI: 10.1124/mol.109.055855
This article has not been copyedited and formatted. The final version may differ from this version.

Abstract

The indolequinone ES936 {5-methoxy-1,2-dimethyl-3-[(4-nitrophenoxy)methyl]indole-4,7-dione} was previously developed in our lab as an antitumor agent against pancreatic cancer. The objective of this study was to identify indolequinones with improved potency against pancreatic cancer and to define their mechanism of action. Pancreatic cancer cell lines PANC-1, MIA PaCa-2, and BxPC-3 were used in *in vitro* assays (MTT and clonogenic assays); indolequinones displayed potent cytotoxicity against all three cell lines and two specific classes of indolequinone were particularly potent agents. These indolequinones induced caspase-dependent apoptosis but no redox cycling or oxidative stress in MIA PaCa-2 and BxPC-3 cells. Selected indolequinones were also screened against the NCI-60 cell line panel and were found to be particularly effective against colon, renal, and melanoma cancer cells. A potential target of these indolequinones was identified as thioredoxin reductase. Indolequinones were found to be potent inhibitors of thioredoxin reductase activity both in pancreatic cancer cells and in cell-free systems. The mechanism of action of the indolequinones was shown to involve metabolic reduction, loss of a leaving group to generate a reactive electrophile resulting in alkylation of the selenocysteine residue in the active site of thioredoxin reductase. *In vivo* efficacy of the indolequinones was also tested in the MIA PaCa-2 pancreatic tumor xenograft in nude mice, and lead indolequinones demonstrated high efficacy and low toxicity. Inhibition of thioredoxin reductase represents a potential novel target in pancreatic cancer and may provide a biomarker of effect of lead indolequinones in this type of cancer.

Molecular Pharmacology Fast Forward. Published on April 13, 2009 as DOI: 10.1124/mol.109.055855
This article has not been copyedited and formatted. The final version may differ from this version.

Introduction

Pancreatic cancer is the fourth leading cause of cancer death in the United States (Jemal et al., 2008) with a 5-year survival rate of <5%. Current treatment options of radiation therapy, chemotherapy, and surgery have been ineffective at improving the survival rate (Ghaneh et al., 2007). Development of novel targeted therapeutic approaches is desperately needed.

We have previously reported the development of an indolequinone, 5-methoxy-1,2-dimethyl-3-[(4-nitrophenoxy)methyl]indole-4,7-dione (ES936, **1**), which exhibited potent growth inhibition effects against human pancreatic cancer cell lines (Dehn et al., 2006). The anti-tumor activity of ES936 was originally attributed to its role as a mechanism-based inhibitor of human NQO1 [NAD(P)H:quinone oxidoreductase 1 (EC 1.6.99.2, DT-diaphorase)] (Winski et al., 2001). NQO1 inhibition by dicumarol, a non-specific inhibitor, has been shown to be cytotoxic in human pancreatic cancer cells (Cullen et al., 2003; Lewis et al., 2004). However, when a series of indolequinone compounds based on ES936 were tested for structure-activity relationship, we found no correlation between the antitumor effects of these indolequinones and NQO1 inhibition in pancreatic cancer cells (Reigan et al., 2007; Colucci et al., 2007). Therefore, the search for alternative molecular targets other than NQO1 is needed to better understand the mechanism of action of these indolequinones against pancreatic cancer.

In the present study, we have developed and examined a series of indolequinones **1-9** (Table 1), based on the structure of ES936. In this paper, we report the antitumor activity of this series of indolequinones against pancreatic cancer cells both *in vitro* and *in vivo*. The

Molecular Pharmacology Fast Forward. Published on April 13, 2009 as DOI: 10.1124/mol.109.055855
This article has not been copyedited and formatted. The final version may differ from this version.

proposed mechanism of action of the indolequinones involves reduction, loss of a leaving group and generation of an electrophile leading to cell death. One potential target of quinone electrophiles is thioredoxin reductase (TrxR; Powis et al., 2006; Chew et al., 2008) and we show in the present study that an established thioredoxin reductase inhibitor had a similar toxicity profile in the NCI-60 panel. Further work employing both purified enzyme and in cancer cells implicated thioredoxin reductase as a potential target of this series of indolequinones.

Molecular Pharmacology Fast Forward. Published on April 13, 2009 as DOI: 10.1124/mol.109.055855
This article has not been copyedited and formatted. The final version may differ from this version.

Materials and methods

Materials

The indolequinones 5-methoxy-1,2-dimethyl-3-[(4-nitrophenoxy)methyl]indole-4,7-dione (ES936, **1**, [Beall et al., 1998]), 6-methoxy-1,2-dimethyl-3-[(4-nitrophenoxy)methyl]indole-4,7-dione (**2**, [Colucci et al., 2007]), 2-hydroxymethyl-5-methoxy-1-methyl-3-[(4-nitrophenoxy)methyl]indole-4,7-dione (**3**, [Newsome, 2004]), 2-hydroxymethyl-5-methoxy-1-methyl-3-[(2,4,6-trifluorophenoxy)methyl]indole-4,7-dione (**4**, [Chilloux, unpublished results]), 2-hydroxymethyl-6-methoxy-1-methyl-3-[(4-nitrophenoxy)methyl]indole-4,7-dione (**5**, [Colucci, 2007]), 6-methoxy-1-methyl-3-[(4-nitrophenoxy)methyl]indole-4,7-dione (**6**, [Colucci, 2007]), 6-methoxy-1-methyl-3-[(2,4,6-trifluorophenoxy)methyl]indole-4,7-dione (**7**, [Colucci, 2007]), 5-methoxy-1-methyl-3-[(4-nitrophenoxy)methyl]indole-4,7-dione (**8**, [Everett et al., 2001]), 5-methoxy-1-methyl-3-[(2,4,6-trifluorophenoxy)methyl]indole-4,7-dione (**9**, [Chilloux, unpublished results]), and 5-methoxy-1,2-dimethyl-3-[1-oxo-2-(2,4,6-trifluorophenyl)ethyl]indole-4,7-dione (ACH983, [Chilloux, unpublished results]) were synthesized according to methods previously developed. Recombinant human NQO2 was obtained from Sigma (St. Louis, MO). Dihydronicotinamide riboside (NRH) was synthesized in our lab using published procedures (Yan et al., 2008; Friedlos et al., 1992). Recombinant rat thioredoxin reductase 1 was purchased from IMCO, Sweden. Rabbit polyclonal antibody against thioredoxin reductase 1 was obtained from Santa Cruz Biotechnology (Santa Cruz, CA). Antibodies

Molecular Pharmacology Fast Forward. Published on April 13, 2009 as DOI: 10.1124/mol.109.055855
This article has not been copyedited and formatted. The final version may differ from this version.

against cleaved caspase 3, 7, 8, 9 are from Cell Signaling Technology (Danvers, MA). Annexin V was obtained from Invitrogene (Carlsbad, CA). Unless indicated, all other chemicals were purchased from Sigma Chemical Co. (St. Louis, MO).

Cell Lines

PANC-1 human pancreatic duct epithelioid carcinoma cells, MIA PaCa-2 human pancreatic carcinoma cells, and BxPC-3 human pancreatic adenocarcinoma cells were obtained from American Type Culture Collection (Manassas, VA). MIA PaCa-2 cells were grown in DMEM adjusted to contain 4 mM L-glutamine, 10% (v/v) fetal bovine serum, 2.5% (v/v) horse serum, 100 units/mL penicillin, and 100 μg/mL streptomycin. PANC-1 and BxPC-3 cells were grown in RPMI 1640 supplemented with 10% (v/v) fetal bovine serum, 2 mM L-glutamine, 100 units/ml penicillin, and 100 μg/mL streptomycin. All cell lines were maintained in a humidified incubator containing 5% carbon dioxide at 37 °C.

Growth Inhibition Assay

Growth inhibition was measured using the MTT colorimetric assay (Mosmann, 1983). In these studies, cells in exponential growth phase were seeded at 2000 cells per well in 96-well plates in triplicate plates and allowed to attach for 16 h. Cells were then treated with indolequinones in complete medium (200 μl/well) for 72 h, or for 4 h followed by incubation in drug free medium (200 μl/well) for additional 72 h at 37 °C. The medium was removed by aspiration, and MTT (50 μg) in complete medium (50 μl) was added to each well and incubated for a further 4 h. Cell viability was determined by measuring the cellular reduction of MTT to the crystalline formazan product which was dissolved by the addition

Molecular Pharmacology Fast Forward. Published on April 13, 2009 as DOI: 10.1124/mol.109.055855
This article has not been copyedited and formatted. The final version may differ from this version.

of 100 μl DMSO. Optical density was determined at 550 nm using a Molecular Devices Thermomax microplate reader. The IC_{50} values were defined as the concentration of indolequinone that resulted in 50% reduction in cell number compared to DMSO treated controls.

Clonogenic Assays

The inhibition of the colony-forming ability of MIA PaCa-2 and BxPC-3 cells by indolequinones was assessed using the clonogenic assay. For these studies, 800 cells were seeded in complete medium into 100 mm tissue culture plates and allowed to attach for 16 h. Cells were then exposed to a concentration range of indolequinones in complete medium for 4 or 72 h. The medium was then replaced with fresh medium and cells incubated at 37 °C for 10 days. Cells were then rinsed in PBS, fixed in 3% (v/v) acetic acid, 10% (v/v) methanol, and stained with 0.2% (w/v) crystal violet, 10% (v/v) formalin in PBS, and colonies were counted manually.

Flow Cytometry Analysis of Apoptosis

MIA PaCa-2 and BxPC-3 cells were seeded at 1×10^5 cells per well in 6-well plates and treated with various concentrations of indolequinone **3** for 4 h followed by incubation in drug-free media for 24 h. Cells were collected, washed with PBS, resuspended in annexin binding buffer (10 mM HEPES, 140 mM NaCl, 2.5 mM $CaCl_2$), and stained with annexin-V and PI according to manufacturers' instructions. Annexin-V and PI staining were determined using flow cytometry with a FACSCalibur (Becton Dickinson). Cells with positive annexin-V staining were counted as apoptotic cells.

Molecular Pharmacology Fast Forward. Published on April 13, 2009 as DOI: 10.1124/mol.109.055855
This article has not been copyedited and formatted. The final version may differ from this version.

Immunoblot Analysis

Cells were seeded in 100 mm culture plates at 6×10^5 cells per plate and treated with various concentrations of indolequinone **3** for 4 h followed by incubation in drug-free media for 24 h. Cells were collected, washed with PBS, and resuspended in caspase lysis buffer [20 mM HEPES, pH 7.5, 10 mM KCl, 1.5 mM $MgCl_2$, 1 mM EDTA, 1 mM EGTA, 1 mM dithiothreitol, 250 mM sucrose, and 0.25 mM phenylmethyl sulfonyl fluoride with protease inhibitors cocktail (Roche Diagnostics, Indianapolis, IN)]. Cells were then sonicated and centrifuged (13,000 rpm × 15 min) and protein concentration of the supernatant was determined using the method of Lowry (Lowry et al., 1951). Cellular proteins (50 μg) were then separated by 12% SDS-PAGE and transferred to PVDF membrane. The membrane was then probed with primary antibodies against caspase-3, 7, 8, 9 and β-actin (Cell Signaling Technology Inc., Beverly, MA) followed by horseradish peroxidase-conjugated goat anti-mouse/rabbit immunoglobulin G secondary antibodies (Jackson ImmunoResearch Laboratories). Western signals were detected using chemiluminescence methods with ECL Western Blotting Detection Reagents (GE Healthcare).

Alkaline Comet Assay

DNA damage was evaluated using the single-cell gel electrophoresis method, commonly known as the alkaline comet assay, as described previously (Tice et al., 2000), including a modified version (Ward et al., 1997) to detect DNA cross-linking. Briefly, cells were seeded in 6-well plates at 1×10^5 cells/well and let attach for 16 h. After 1 h drug treatment, cells were harvested and 1×10^4 cells were then subjected to the comet assay. Comet slides

Molecular Pharmacology Fast Forward. Published on April 13, 2009 as DOI: 10.1124/mol.109.055855
This article has not been copyedited and formatted. The final version may differ from this version.

were stained with PI and viewed using fluorescence microscopy under a Nikon invert microscope (Nikon Eclipse TE300) at 20× magnification. Images were captured using an attached CoolSNAP$_{ES}$ CCD camera. One hundred cells, 50 each on duplicate slides were captured and scored using a software package (Komet Version 5, Kinetic Imaging, Belfast, UK). The percent of DNA in comet tail was recorded for each comet as an indication of the extent of DNA single strand breaks.

For measurement of DNA cross-linking, a fixed amount of single strand breaks was induced post-treatment into control and indolequinone-treated cells at each concentration point by incubating with 200 μM H_2O_2 for 20 min on ice. Cross-linked DNA is unable to migrate from the head of the comet, and the extent of DNA cross-linking can be indirectly measured by analyzing the relative reduction of DNA migration induced by H_2O_2 compared with untreated H_2O_2 controls.

Thioredoxin reductase activity in cells

Cells were seeded in 100 mm culture plates at 6 × 10^5 cells per plate and treated with various concentrations of indolequinones for 4 h; cells were then collected in RIPA buffer, sonicated, centrifuged (13,000 rpm × 15 min) and protein concentration in supernatant was determined using the method of Lowry. Thioredoxin reductase activity assay was then performed in 96-well plates using an endpoint insulin reduction assay as previously described (Fang et al., 2005). Briefly, reactions (50 μl) contained 50 mM Tris-HCl (pH 7.4), 2 mM EDTA, 200 μM NADPH, 1.5 mg/ml insulin, 20 μM *E. coli* Trx, and 40 μg of protein from each cell extract. After incubation for 20 min at 37 °C, the reaction was terminated by adding 200 μl of 1 mM DTNB in 6 M guanidine hydrocholoride (dissolved in 50 mM

Molecular Pharmacology Fast Forward. Published on April 13, 2009 as DOI: 10.1124/mol.109.055855
This article has not been copyedited and formatted. The final version may differ from this version.

Tris-HCl, pH 8.0). The free thiols of the reduced insulin were determined by DTNB reduction, measured by the absorbance at 412 nm, where 1 mol of disulfide give rise to 2 mol of free TNB with the extinction coefficient 13.6 $mM^{-1} \cdot cm^{-1}$. A blank measurement for each sample, containing everything except Trx, was treated in the same manner, and the blank value was subtracted from the corresponding absorbance value of the sample. The activity of TrxR was expressed as the percentage of DMSO treated control.

Inhibition of Thioredoxin Reductase in Cell-free System

Inhibition reaction was carried out in 100 mM potassium phosphate buffer (pH 7.4), containing 2 mM EDTA and 1 mg/ml BSA. A mixture of 0.5 μM recombinant rat TrxR, 250 μM NADPH, 2 μM NQO2, and 200 μM NRH were incubated in the above buffer at room temperature for 5 min. Then various concentrations of indolequinone were added (the final volume of the mixture was 150 μl) and a 20 μl sample was removed every 5 min up to 30 min and measured for TrxR activity using the DTNB reduction assay, as previously described (Fang et al., 2005). The TrxR activity assay mixture contains 100 mM potassium phosphate buffer (pH 7.4), 2 mM EDTA, 1 mg/ml BSA, 250 μM NADPH, and 2.5 mM DTNB. The release of TNB from DTNB was monitored at 412 nm for 1 min after sample addition and the rate calculated and a blank reading without samples was subtracted from every sample. Results were expressed as percent of control (20 μl sample removed before addition of IQs) and were representative of three separate experiments.

Detection of Indolequinone-modified Residues in TrxR using Biotin-conjugated Iodoacetamide

Molecular Pharmacology Fast Forward. Published on April 13, 2009 as DOI: 10.1124/mol.109.055855
This article has not been copyedited and formatted. The final version may differ from this version.

The free selenocysteine in TrxR was detected as previously reported (Chew et al., 2008). TrxR was incubated with increasing concentrations of indolequinone **3** under identical conditions as in the pure enzyme inhibition assay. After 5 min incubation at room temperature, 1 μl of reaction mixture was taken out and mixed with 19 μl of 100 μM biotin-conjugated iodoacetamide (BIAM, pH 6.5) and incubated at 37°C for another 30 min to alkylate the free –SeH groups in the enzyme. The products were then separated by 10% SDS-PAGE and transferred to PVDF membrane. Proteins labeled with BIAM were detected with horseradish peroxidase-conjugated strepavidin and enhanced chemiluminescence detection.

Indolequinone Antitumor Activity in Human Pancreatic Xenograft Tumors

All experiments were approved by the University of Colorado Denver Animal Care and Use Committee and were carried out according to approved protocols. Female athymic nude mice (Ncr *nu/nu*; National Cancer Institute, Fredrick, MD) were received at 5 to 6 weeks of age and were allowed to acclimate for 2 weeks in sterile microisolator cages with constant temperature and humidity. Mice had free access to food and water. MIA PaCa-2 cells in log-phase growth were harvested on the day of use. Cells were suspended in 75:25 unsupplemented medium/Matrigel and 0.1 mL (2×10^7 cells) was injected s.c. into the right flank of each animal. After inoculation of tumor cells, mice were monitored daily, weighed twice weekly and digital caliper measurements were begun when tumors became visible. When tumors had grown to ~200 mm^3 (~12 days after implantation), tumor-bearing mice were randomized into control and drug treatment groups. For these studies, the indolequinones (dissolved in 100% sterile DMSO) were injected i.p. every other day for 20

Molecular Pharmacology Fast Forward. Published on April 13, 2009 as DOI: 10.1124/mol.109.055855
This article has not been copyedited and formatted. The final version may differ from this version.

days at the dose of 1.0 or 2.5 mg/kg. No obvious toxicities or weight loss were observed in the control (DMSO) or indolequinone-treated animals during treatment. Tumor volume was calculated by the formula $(L \times W^2) / 2$, where L is the longer measurement of the tumor and W is the smaller tumor measurement. T/C (ratios of tumor volumes of treated and control tumors as an indicator of drug efficacy) were calculated as previously described (Dehn et al., 2006).

Statistical analysis

Statistical analysis was performed using one-way analysis of variance followed by appropriate post hoc tests: Dunnett test for comparison of multiple observations to a single control; Student's t test for pairwise comparisons. Data are represented as mean ± standard deviation of at least three replicate experiments.

Molecular Pharmacology Fast Forward. Published on April 13, 2009 as DOI: 10.1124/mol.109.055855
This article has not been copyedited and formatted. The final version may differ from this version.

Results

Growth Inhibitory Activity of the Indolequinones in Human Pancreatic Cancer Cell Lines

The effect of the indolequinones on the growth of human pancreatic cancer cells was assessed using the MTT assay in PANC-1, MIA PaCa-2, and BxPC-3 pancreatic cancer cell lines following 4 or 72 h treatment with the indolequinones and the IC_{50} values in each cell line are listed in Table 2. In all three cell lines, the indolequinones exhibited marked growth inhibitory activity. A structure-activity relationship was observed and this series of indolequinones can be subdivided into three classes by the substituent on the 2-position of the indole ring. The order of potency of the indolequinones was 2-unsubstituted class (**6-9**) > 2-hydroxymethyl class (**3-5**) > 2-methyl class (**1, 2**).

Cytotoxic Activity of the Indolequinones in Pancreatic Cancer Cell Lines

In order to confirm the growth inhibition data obtained using the mitochondria-based MTT assay, the effect of the indolequinones in human pancreatic cancer cell lines was also assessed using the clonogenic assay. The colony-forming ability was measured in MIA PaCa-2 (indolequinones **1-8**) and BxPC-3 (**1-4, 8, 9**) cells following 4 or 72 h treatment with the indolequinones (Figure 1). A similar order of potency, as in the MTT assay, was observed for the three classes of indolequinones.

Induction of Caspase-dependent Apoptosis by the Indolequinones in Pancreatic Cancer Cell Lines

The ability of the indolequinones to induce apoptotic cell death was measured in MIA

Molecular Pharmacology Fast Forward. Published on April 13, 2009 as DOI: 10.1124/mol.109.055855
This article has not been copyedited and formatted. The final version may differ from this version.

PaCa-2 and BxPC-3 cells using flow cytometry analysis. A dose-dependent increase in apoptosis was observed in both MIA PaCa-2 and BxPC-3 cells (Figure 2A) following indolequinone **3** treatment (24 h), at concentration ranges around the MTT IC_{50} values. The indolequinone **3**-induced apoptosis could be completely blocked by the pan-caspase inhibitor z-VAD-fmk (Figure 2B), suggesting that apoptosis is caspase-dependent. In fact, caspase-3, 7, 8, 9 activation was detected in both cell lines after 24 h drug treatment using immunoblot analysis (Figure 2C). There was a dose-dependent increase in the amount of the cleaved form of caspase 3 (17/19 kDa), caspase 7 (20 kDa), caspase 8 (18 kDa), and caspase 9 (35/37 kDa) in both cell lines.

Effect of Indolequinone Treatment on DNA Single Strand Breaks and DNA Cross-Links in Pancreatic Cancer Cell Lines

The ability of the indolequinones to induce DNA damage, including both DNA single strand breaks and DNA cross-linking, was measured in MIA PaCa-2 and BxPC-3 cell lines using the Comet Assay. In Fig. 3A, the percent of DNA in the comet tail was recorded as an indication of the extent of DNA single strand breaks. H_2O_2 treatment as a positive control induced significant amounts of DNA single strand breaks in both cell lines; no significant DNA single strand breaks could be observed in either cell line following 1 h of indolequinone **3** treatment. In Fig. 3B, indolequinone-induced DNA single strand breaks were compared with two known redox cycling quinones β-lapachone and streptonigrin. The lack of DNA single strand breaks relative to the redox cycling quinones suggest that the indolequinone compounds do not induce significant redox cycling and oxidative stress. In Fig. 3C, the extent of DNA crosslinking caused by indolequinone treatment was indirectly

Molecular Pharmacology Fast Forward. Published on April 13, 2009 as DOI: 10.1124/mol.109.055855
This article has not been copyedited and formatted. The final version may differ from this version.

measured by analyzing the relative reduction of H_2O_2-induced DNA migration into the comet tail compared with drug untreated H_2O_2 control. The fact that there was no significant difference in percent tail DNA among all the treatment groups indicated that indolequinone treatment did not result in measurable DNA cross-links in either cell line. Indolequinone-induced DNA damage was also monitored at later time points (up to 4 h); DNA strand breaks were detectable concomitant with apoptosis using both COMET and γH2AX histone blotting (data not shown), using high concentrations of compounds (>500 nM) above the MTT and clonogenic IC_{50} values.

Antitumor Activity Profile of the Indolequinones in the NCI-60 Tumor Cell Line Panel

Selected indolequinone compounds were screened in the Molecular Cancer Therapeutics Program NCI-60 tumor cell line panel. Indolequinones **2, 3, 6,** representative of the 2-methyl, 2-hydroxymethyl, and 2-unsubstituted indolequinone classes, respectively, were found to have potent anti-proliferative activities particularly against renal, colorectal, and melanoma cancers (Figure 4, the results for **3** and **6** are shown, the result for **2** is similar). Interestingly, this unique pattern of antitumor activity is very similar to that of AW464 (Figure 4), an antitumor quinol compound (Bradshaw et al., 2005) which has been proven to be a potent inhibitor of the thioredoxin reductase/thioredoxin system. In recent work, AW464 and its derivatives were shown to preferentially target thioredoxin reductase rather than thioredoxin (Chew et al., 2008). The similarity in the pattern of antitumor activity (NCI-60) between our compounds and AW464 suggested that thioredoxin reductase might be a critical target of these indolequinones.

Molecular Pharmacology Fast Forward. Published on April 13, 2009 as DOI: 10.1124/mol.109.055855
This article has not been copyedited and formatted. The final version may differ from this version.

Inhibition of Thioredoxin Reductase by Indolequinones in Human Tumor Cell Lines

The ability of indolequinone **3** (2-hydroymethyl class) and **9** (2-unsubstituted class) to inhibit thioredoxin reductase activity was tested in the human pancreatic cancer cell line MIA PaCa-2 following 4 h drug treatment. Thioredoxin reductase activity was measured in these cells using the endpoint insulin reduction assay (Fang et al., 2005). A dose-dependent inhibition of thioredoxin reductase activity was observed for both IQ **3** and IQ **9** (Figure 5A)**.** In consistent with the cytotoxicity data, IQ **9,** which was more toxic to pancreatic cancer cells than IQ **3**, was more potent at inhibiting TrxR activity in cells. The I_{50} value for TrxR inhibition was 146 nM for IQ **3** and 82 nM for IQ **9**, respectively. In contrast, an indolequinone analogue (designated ACH983; structure shown in Figure 5A) which is incapable of expelling a leaving group after reduction and which does not induce growth inhibition in MIA PaCa-2 cells was not able to inhibit TrxR in MIA PaCa-2 cells. A growth inhibitory IC_{50} (MTT) for ACH983 could not be determined because of a lack of growth inhibitory effect at concentrations up to 5 μM.

Inhibition of Thioredoxin Reductase by Indolequinone 3 in Cell Free System

The ability of indolequinone **3** to inhibit recombinant rat TrxR was tested in cell free system using NQO2/NRH as the reductive activation step (indolequinones tested did not inhibit NQO2 activity under these conditions). When NADPH-reduced TrxR was incubated with NQO2/NRH reduced IQ **3**, a dose-dependent inhibition of TrxR activity was observed (Figure 5B, open square). The indolequinone-induced inactivation of TrxR was fast; maximum inhibition was achieved 5 min after addition of compound. Inhibition was NADPH-dependent since the activity of non-reduced TrxR (no preincubation with NADPH)

Molecular Pharmacology Fast Forward. Published on April 13, 2009 as DOI: 10.1124/mol.109.055855
This article has not been copyedited and formatted. The final version may differ from this version.

was not affected by NQO2/NRH reduced IQ **3** (Figure 5B, open triangle), suggesting that the selenocysteine active site of the enzyme was involved in the inhibition by indolequinones. The indolequinone compound also has to be reduced for the inhibition to occur since the enzyme activity of TrxR was unaffected in the absence of NQO2/NRH (Figure 5B, closed triangle), indicating that the toxic species responsible for TrxR inhibition was generated after reduction and ejection of the leaving group. The inhibition of TrxR appeared to be irreversible, since desalting of the inhibited TrxR enzyme did not result in recovery of enzyme activity up to 24 h after initial inhibition.

Detection of the TrxR Selenocysteine Redox-active Site as the Potential Target for Indolequinone Modification

To test whether the IQs were inhibiting TrxR through modification of the selenocysteine active site, the biotin-conjugated iodoacetamide (BIAM) alkylation assay was carried out to probe the amount of free –SeH groups in the enzyme after inhibition by indolequinone **3**. BIAM has been shown to preferentially alkylate with selenocysteine at pH 6.5 (Chew et al., 2008). A dose-dependent decrease in the amount of free selenocysteine in TrxR was observed following incubation with reduced indolequinone (Figure 5 C), suggesting that the indolequinones attack the selenocysteine in the active site, resulting in irreversible inhibition of TrxR.

Antitumor Effects of the Indolequinones in Pancreatic Tumor Xenografts

The *in vivo* antitumor activity of the indolequinones against pancreatic cancer was tested using MIA PaCa-2 xenograft tumors implanted into nude mice. For these studies, the most

Molecular Pharmacology Fast Forward. Published on April 13, 2009 as DOI: 10.1124/mol.109.055855
This article has not been copyedited and formatted. The final version may differ from this version.

active indolequinones in cellular assays compounds **8, 9** were dosed at 1.0 and 2.5 mg/kg (i.p.) every other day for 20 days. Tumor volumes were calculated from control and indolequinone-treated mice during drug treatment. Compounds **8, 9** induced marked growth inhibition of the MIA PaCa-2 xenograft in a dose dependent manner (Figure 6). The optimal T/C ratio based on tumor volume analysis was 25.2 % for indolequinone **9** in the 2.5 mg/Kg group.

Molecular Pharmacology Fast Forward. Published on April 13, 2009 as DOI: 10.1124/mol.109.055855
This article has not been copyedited and formatted. The final version may differ from this version.

Discussion

ES936 and analogs were developed in our lab originally as mechanism-based inhibitors of NQO1. After reduction to the hydroquinone form by NQO1, ES936 loses the *p*-nitrophenol leaving group from the indole 3-position and the iminium ion generated subsequently reacts with tyrosine residues in the active site of NQO1, resulting in the inhibition of enzymatic activity (Winski et al., 2001). ES936 and analogs were found to be active against human pancreatic cancer (Dehn et al., 2006); however, the antitumor activity of ES936 and analogues did not correlate with their ability to inhibit NQO1 (Reigan et al., 2007; Colucci et al., 2007). We corroborated this finding in the current study using three different classes of indolequinone analogs. The 2-hydroxymethyl and 2-unsubstituted indolequinones, which are much poorer inhibitors of NQO1 compared to the 2-methyl indolequinone ES936 (unpublished data), were markedly more toxic to pancreatic cancer cell lines *in vitro*; and the 2-H derivatives which were tested in xenografts were more active than ES936 which was tested in a previous study (Dehn et al., 2006). The dissociation of anti-tumor activity from NQO1 inhibition suggests that other molecular targets are involved in the antitumor activity of this indolequinone series.

A clear structure-activity relationship was observed amongst the indolequinones tested. Variation in the substituent on the 2-position of the indole ring had a marked effect on the antitumor potency of the indolequinones. The ES936 class (2-methyl) is the least active; the 2-hydroxymethyl class is several fold more potent; and the 2-unsubstituted class is the most active at inducing growth inhibition of pancreatic tumor cells. Indolequinones of the 2-hydroxymethyl class (compound **3** as prototype) are more water-soluble than either the

Molecular Pharmacology Fast Forward. Published on April 13, 2009 as DOI: 10.1124/mol.109.055855
This article has not been copyedited and formatted. The final version may differ from this version.

2-methyl class or the 2-unsubstituted classes, which may be an advantage in future drug development.

Indolequinone-induced cytotoxicity in pancreatic cancer cell lines was mediated by apoptotic cell death. A dose dependent increase in apoptosis was induced by indolequinone **3** treatment in both MIA PaCa-2 and BxPC-3 cells at drug concentrations around the IC_{50} values (Figure 2 A-B). This was confirmed by the detection of cleaved caspase 3 and 7 (executioner caspases) in both cell lines (Figure 2C). The fact that both caspase 8 (extrinsic pathway of apoptosis) and caspase 9 (intrinsic pathway of apoptosis) were activated implied a crosstalk between the two major signaling pathways of apoptosis. However, treatment with the indolequinones did not induce increased levels of superoxide in pancreatic cancer cells (data not shown), suggesting that the indolequinones do not induce oxidative stress. In addition, no significant DNA damage, either single strand breaks or DNA cross-links (COMET assay), was observed in MIA PaCa-2 or BxPC-3 pancreatic cancer cell lines after 1 h indolequinone treatment (Figure 3A). The lack of single strand break induction relative to known redox cycling quinones such as β-lapachone and streptonigrin (Figure 3B) further confirmed the absence of indolequinone-induced oxidative stress. However, DNA strand breaks were detectable at later time points concomitant with apoptosis using both COMET and γH2AX histone blotting, but only at high drug concentrations above MTT and clonogenic IC_{50} values. These observations suggested that the cytotoxicity and caspase-dependent apoptosis observed in our study were not caused by redox cycling and oxidative stress.

Molecular Pharmacology Fast Forward. Published on April 13, 2009 as DOI: 10.1124/mol.109.055855
This article has not been copyedited and formatted. The final version may differ from this version.

In an attempt to elucidate potential molecular targets of the indolequinones, three indolequinone compounds **2, 3, 6**, one from each of the three 2-substitued classes of compound, were screened against the NCI-60 cell line panel and a distinct pattern of antitumor activity was revealed (Figure 4). The indolequinones tested were particularly effective against colon, renal, and melanoma cancer cells (the NCI-60 does not contain a pancreatic sub-panel). Interestingly, this pattern of activity is very similar to that of AW464, an antitumor quinol compound which has recently been established as a thioredoxin reductase inhibitor (Bradshaw et al., 2005; Chew et al., 2008). The thioredoxin system, consisting of thioredoxin (Trx), thioredoxin reductase (TrxR), and NADPH, plays an essential role in maintaining the redox state of thiols in cellular proteins (Arnér and Holmgren, 2006). The mammalian thioredoxin reductases are selenium-containing flavoproteins with a C-terminal Cys-selenocysteine active site essential for its redox activity (Gromer et al., 1998). Thioredoxin is reduced at the free selenocysteine site of TrxR which is generated when TrxR is reduced by NADPH. Reduced thioredoxin can promote proliferation, inhibit apoptosis and protect cells against oxidative stress (Powis and Montfort, 2001). TrxR has emerged as an important target for cancer chemotherapy recently, since the level of TrxR and thioredoxin has been shown to be elevated in a variety of human cancer types (Urig and Becker, 2006). TrxR and Trx overexpression have been associated with enhanced tumor proliferation, decreased apoptosis, increased angiogenesis, increased resistance to chemotherapeutic drugs and reduced survival.

Several antitumor compounds known to generate electrophiles have been shown to be inhibitors of TrxR (Fang et al., 2005; Bradshaw et al., 2005; Chew et al., 2008; Nordberg et

Molecular Pharmacology Fast Forward. Published on April 13, 2009 as DOI: 10.1124/mol.109.055855
This article has not been copyedited and formatted. The final version may differ from this version.

al., 1998; Witte et al., 2005; Lu et al., 2007; Kirkpatrick et al., 1998; Wipf et al., 2004). The selenocysteine of thioredoxin reductase has been shown to be very vulnerable to electrophilic attack because of its low pKa and marked reactivity relative to cysteine residues (Arnér and Holmgren, 2006). Alkylation and inhibition of thioredoxin reductase by electrophiles could result in the induction of cell death by affecting the redox state of thioredoxin and other downstream cellular proteins (Lu et al., 2007). Alternatively, in recent work alkylated thioredoxin reductase has been shown to have an altered functionality in cancer cells and can drive apoptosis (Anestål and Arnér, 2003; Cassidy et al., 2006). The reduction of the indolequinones by cellular reductases results in the ejection of the leaving group and the generation of an electrophilic alkylating species. Several pieces of data support thioredoxin reductase as a potential target of the indolequinones. First, indolequinone **3** and **9** were found to inhibit TrxR activity in MIA PaCa-2 cells in a dose-dependent manner, suggesting that the indolequinones were capable of inhibiting thioredoxin reductase in tumor cells at drug concentrations approximating IC_{50} values. Importantly, the more toxic compound IQ **9** is more potent than IQ **3** at inhibiting TrxR in cells. Second, the indolequinone ACH983 which does not have a leaving group and was nontoxic had no effect on TrxR activity in cells, suggesting that inhibition of TrxR activity is related to the growth-inhibitory effect of the indolequinones and that the ejection of the leaving group is a prerequisite for activity of the indolequinones. Third, indolequinone **3** was also shown to irreversibly inhibit thioredoxin reductase activity in cell free systems, but only after bioreductive activation by NQO2/NRH, suggesting that a reduction step is needed and that the toxic species are generated after reduction and ejection of the leaving group. The observation that inhibition of TrxR was NADPH-dependent and irreversible

Molecular Pharmacology Fast Forward. Published on April 13, 2009 as DOI: 10.1124/mol.109.055855
This article has not been copyedited and formatted. The final version may differ from this version.

suggested that the free selenocysteine active site of TrxR generated via NADPH-mediated reduction was the potential target of indolequinone-derived electrophiles. This was further confirmed by the BIAM alkylation method which showed the loss of the free selenocysteine residue in the active site of recombinant TrxR after incubation of reduced IQs. A proposed mechanism of TrxR inhibition by the indolequinones is summarized in Figure 7.

In conclusion, we have examined three classes of indolequinone compounds which differ in antitumor potency. All three classes of indolequinones displayed potent antitumor activity against pancreatic tumor cells *in vitro*; compounds in the most active 2-H class demonstrated marked activity against the MIA PaCa-2 xenograft *in vivo*. The cytotoxicity of the indolequinones in pancreatic cancer cells was mediated by caspase activation and apoptotic cell death. Importantly, the indolequinones were found to inhibit thioredoxin reductase activity both in cells and in cell free systems, providing a possible explanation for the molecular mechanism of action of the indolequinone series. Validation of thioredoxin reductase as the molecular target of these indolequinone compounds is currently underway.

References

Anestål K, Arnér ES (2003) Rapid induction of cell death by selenium-compromised thioredoxin reductase 1 but not by the fully active enzyme containing selenocysteine. *J Biol Chem* **278:** 15966-72.

Arnér ES, Holmgren A (2006). The thioredoxin system in cancer. *Semin Cancer Biol* **16:** 420-6.

Beall HD, Winski S, Swann E, Hudnott AR, Cotterill AS, O'Sullivan N, Green SJ, Bien R, Siegel D, Ross D, Moody CJ (1998) Indolequinone antitumor agents: correlation between quinone structure, rate of metabolism by recombinant human NAD(P)H:quinone oxidoreductase, and in vitro cytotoxicity. *J Med Chem* **41:** 4755-66.

Bradshaw TD, Matthews CS, Cookson J, Chew EH, Shah M, Bailey K, Monks A, Harris E, Westwell AD, Wells G, Laughton CA, Stevens MF (2005) Elucidation of thioredoxin as a molecular target for antitumor quinols. *Cancer Res* **65:** 3911-9.

Cassidy PB, Edes K, Nelson CC, Parsawar K, Fitzpatrick FA, Moos PJ (2006) Thioredoxin reductase is required for the inactivation of tumor suppressor p53 and for apoptosis induced by endogenous electrophiles. *Carcinogenesis* **27:** 2538-49.

Chew EH, Lu J, Bradshaw TD, Holmgren A (2008) Thioredoxin reductase inhibition by antitumor quinols: a quinol pharmacophore effect correlating to antiproliferative activity.

FASEB J **22:** 2072-83.

Colucci MA (2007) PhD Thesis, University of Nottingham, Nottingham, UK.

Colucci MA, Reigan P, Siegel D, Chilloux A, Ross D, Moody CJ (2007) Synthesis and evaluation of 3-aryloxymethyl-1,2-dimethylindole-4,7-diones as mechanism-based inhibitors of NAD(P)H:quinone oxidoreductase 1 (NQO1) activity. *J Med Chem* **50:** 5780-9.

Dehn DL, Siegel D, Zafar KS, Reigan P, Swann E, Moody CJ, Ross D (2006) 5-Methoxy-1,2-dimethyl-3-[(4-nitrophenoxy)methyl]indole-4,7-dione, a mechanism-based inhibitor of NAD(P)H:quinone oxidoreductase 1, exhibits activity against human pancreatic cancer in vitro and in vivo. *Mol Cancer Ther* **7:**1702-9.

Everett SA, Naylor MA, Barraja P, Swann E, Patel KB, Stratford MRL, Hudnott AR, Vojnovic B, Locke RJ, Wardman P, Moody CJ (2001) Controlling the rates of reductively activated elimination from the (indol–3–yl)methyl position of indolequinones. *J. Chem. Soc., Perkin Trans. 2* 843-860.

Fang J, Lu J, Holmgren A (2005) Thioredoxin reductase is irreversibly modified by curcumin: a novel molecular mechanism for its anticancer activity. *J Biol Chem* **280:** 25284-90.

Friedlos F, Jarman M, Davies LC, Boland MP, Knox RJ (1992) Identification of novel reduced pyridinium derivatives as synthetic co-factors for the enzyme DT diaphorase (NAD(P)H dehydrogenase (quinone), EC 1.6.99.2). *Biochem Pharmacol.* **44:**25-31.

Ghaneh P, Costello E, Neoptolemos JP (2007) Biology and management of pancreatic cancer. *Gut* **56:** 1134-52.

Gromer S, Arscott LD, Williams CH Jr, Schirmer RH, Becker K (1998) Human placenta thioredoxin reductase. Isolation of the selenoenzyme, steady state kinetics, and inhibition by therapeutic gold compounds. *J Biol Chem* **273:** 20096-101.

Jemal A, Siegel R, Ward E, Hao Y, Xu J, Murray T, Thun MJ (2008) Cancer statistics, 2008. *CA Cancer J Clin* **58:** 71-96.

Kirkpatrick DL, Kuperus M, Dowdeswell M, Potier N, Donald LJ, Kunkel M, Berggren M, Angulo M, Powis G (1998) Mechanisms of inhibition of the thioredoxin growth factor system by antitumor 2-imidazolyl disulfides. *Biochem Pharmacol* **55:** 987-94.

Lowry OH, Rosebrough NJ, Farr AL, Randall RJ (1951) Protein measurement with the Folin phenol reagent. *J Biol Chem* **193:** 265-75.

Lu J, Chew EH, Holmgren A (2007) Targeting thioredoxin reductase is a basis for cancer therapy by arsenic trioxide. *Proc Natl Acad Sci USA* **104:** 12288-93.

Mosmann T (1983) Rapid colorimetric assay for cellular growth and survival: application to proliferation and cytotoxicity assays. *J Immunol Methods* **65:** 55-63.

Newsome JJ (2004) PhD Thesis, University of Exeter, Exeter, UK.

Nordberg J, Zhong L, Holmgren A, Arnér ES (1998) Mammalian thioredoxin reductase is irreversibly inhibited by dinitrohalobenzenes by alkylation of both the redox active selenocysteine and its neighboring cysteine residue. *J Biol Chem* **273:** 10835-42.

Powis G, Montfort WR (2001) Properties and biological activities of thioredoxins. *Annu Rev Pharmacol Toxicol* **41:** 261-95.

Powis G, Wipf P, Lynch SM, Birmingham A, Kirkpatrick DL (2006) Molecular pharmacology and antitumor activity of palmarumycin-based inhibitors of thioredoxin reductase. *Mol Cancer Ther* **5:**630-6.

Reigan P, Colucci MA, Siegel D, Chilloux A, Moody CJ, Ross D (2007) Development of indolequinone mechanism-based inhibitors of NAD(P)H:quinone oxidoreductase 1 (NQO1): NQO1 inhibition and growth inhibitory activity in human pancreatic MIA PaCa-2 cancer cells. *Biochemistry* **46:** 5941-50.

Tice RR, Agurell E, Anderson D, Burlinson B, Hartmann A, Kobayashi H, Miyamae Y, Rojas E, Ryu JC, Sasaki YF (2000) Single cell gel/comet assay: guidelines for in vitro and

in vivo genetic toxicology testing. *Environ Mol Mutagen* **35:** 206-21.

Urig S, Becker K (2006) On the potential of thioredoxin reductase inhibitors for cancer therapy. *Semin Cancer Biol* **16:** 452-65.

Ward TH, Butler J, Shahbakhti H and Richards JT (1997) Comet assay studies on the activation of two diaziridinylbenzoquinones in K562 cells. *Biochem Pharmacol* **53:** 1115–1121.

Winski SL, Faig M, Bianchet MA, Siegel D, Swann E, Fung K, Duncan MW, Moody CJ, Amzel LM, Ross D (2001) Characterization of a mechanism-based inhibitor of NAD(P)H:quinone oxidoreductase 1 by biochemical, X-ray crystallographic, and mass spectrometric approaches. *Biochemistry* **40:** 15135-42.

Wipf P, Lynch SM, Birmingham A, Tamayo G, Jiménez A, Campos N, Powis G (2004) Natural product based inhibitors of the thioredoxin-thioredoxin reductase system. *Org Biomol Chem* **2:** 1651-8.

Witte AB, Anestål K, Jerremalm E, Ehrsson H, Arnér ES (2005) Inhibition of thioredoxin reductase but not of glutathione reductase by the major classes of alkylating and platinum-containing anticancer compounds. *Free Radic Biol Med* **39:** 696-703.

Yan C, Kepa JK, Siegel D, Stratford IJ, Ross D (2008) Dissecting the role of multiple

reductases in bioactivation and cytotoxicity of the antitumor agent 2,5-diaziridinyl-3-(hydroxymethyl)-6-methyl-1,4-benzoquinone (RH1). *Mol Pharmacol* 74:1657-65.

Molecular Pharmacology Fast Forward. Published on April 13, 2009 as DOI: 10.1124/mol.109.055855
This article has not been copyedited and formatted. The final version may differ from this version.

Footnotes

Grant support: This research was supported by NIH [Grant RO1 CA-114441] (DR), and by grants from FORCE (Exeter) and the Association for International Cancer Research to C.J.M.

Request for reprints: David Ross, Department of Pharmaceutical Sciences, School of Pharmacy, University of Colorado Denver, C-238, 12700 East 19th Avenue, Aurora, CO 80045, USA. Phone: 330-724-7265; Fax: 303-724-7266. Email: david.ross@ucdenver.edu

Molecular Pharmacology Fast Forward. Published on April 13, 2009 as DOI: 10.1124/mol.109.055855
This article has not been copyedited and formatted. The final version may differ from this version.

Legends for figures

Figure 1. Effect of indolequinone treatment on colony formation in human pancreatic cancer cells. Colony forming ability was measured in MIA PaCa-2 and BxPC-3 cells following 4 or 72 h indolequinone treatment. Data represent mean ± standard deviation of three independent determinations.

Figure 2. Induction of caspase-dependent apoptosis by indolequinone 3 in pancreatic cancer cells. (A) Effect of indolequinone **3** treatment on apoptotic cell death. MIA PaCa-2 and BxPC-3 cells were treated with indolequinone **3** at various concentrations. Apoptosis was measured 24 h after 4 h drug treatment using annexin-PI staining in combination with flow cytometry analysis. **(B)** Effect of pretreatment with the pan-caspase inhibitor z-VAD-fmk on indolequinone **3**-induced apoptosis. BxPC-3 cells were pretreated with 100 μM z-VAD-fmk for 30 min before indolequinone **3** treatment. Data represent mean ± standard deviation of three independent determinations. **(C)** Induction of caspase activation by indolequinone 3 in MIA PaCa-2 and BxPC-3 pancreatic cancer cells. The cleaved forms of caspase 3, 7, 8, 9 were detected in both cell lines using immunoblot analysis 24 h after 4 h drug treatment. Staurosporine (STAU) treatment (500nM) was included as positive control for caspase activation. Immunoblot shown was representative of at least three independent experiments.

Figure 3. Effect of indolequinone 3 treatment on DNA single strand breaks and DNA cross-links in MIA PaCa-2 and BxPC-3 cells. DNA damage was determined using the

Molecular Pharmacology Fast Forward. Published on April 13, 2009 as DOI: 10.1124/mol.109.055855
This article has not been copyedited and formatted. The final version may differ from this version.

comet assay after treating cells with varying concentrations of indolequinone **3** (IQ3) for 1 h. (A) DNA single strand breaks were expressed as percentage of DNA in the comet tail. H_2O_2 treatment (200 μM for 20 min) was included as a positive control. (B) Comparison of drug-induced DNA single strand breaks in MIA PaCa-2 cells between indolequinone **3** and known redox cycling quinones β-lapachone (β-lap) and streptonigrin (SN). Cells were treated for 1 h. The dose range used for β-lapachone was 1-10 μM. (C) No DNA cross-links were observed following 1 h indolequinone **3** treatment since there was no decrease in percent tail DNA in drug-treated cells compared to untreated H_2O_2 control. Results are expressed as the mean ± standard deviation of three separate determinations. ** Significantly different from non-treatment control cells, $p < 0.01$

Figure 4. Anti-tumor Activity of indolequinones in the NCI-60 Cell Line Panel. Growth inhibition screening in the NCI-60 cell line panel was performed by the NCI/NIH developmental therapeutics program. The LC_{50} mean graph was compared side-by-side for compound **3** (left), **6** (middle), and AW464, a recently established thioredoxin reductase inhibitor (right). The original graph for compound **3** and **6** were obtained from NCI; the AW464 part of this figure was adapted from a recently published paper (Bradshaw et al., 2005).

Figure 5. Inhibition of thioredoxin reductase activity by indolequinone 3. (A) Inhibition of thioredoxin reductase activity in MIA PaCa-2 cells by indolequinone **3** (▲), indolequinone **9** (▽), and a non-toxic indolequinone analog ACH983 (▼). Thioredoxin reductase activity in MIA PaCa-2 cells was measured using the endpoint insulin reduction

Molecular Pharmacology Fast Forward. Published on April 13, 2009 as DOI: 10.1124/mol.109.055855
This article has not been copyedited and formatted. The final version may differ from this version.

assay following 4 h of drug treatment. Data were expressed as percent of DMSO-treated control. Data represent mean ± standard deviation of three independent determinations. **(B)** Inhibition of thioredoxin reductase activity in cell-free system by indolequinone **3**. Recombinant rat TrxR (0.5μM) was pre-incubated for 5 min with 250 μM NADPH in the presence of NQO2/NRH, then indolequinone **3** was added and incubated for 5 min (maximum inhibition was achieved at 5 min). An aliquot of 20 μl sample was taken out for measurement of TrxR activity using DTNB as substrate. □, reaction system contained every component; △, non-reduced TrxR (-NADPH) was not inhibited; ▼, non-reduced indolequinone **3** (-NQO2/NRH) resulted in no inhibition. **(C)** Alkylation of the C-terminal selenocysteine of recombinant rat TrxR by indolquinone **3** following reduction by NQO2/NRH inhibited subsequent biotinylation of the C-terminal selenocysteine by biotinylated iodoacetamide. Top panel: biotinylation of TrxR was detected using strepavidin-conjugated HRP in combination with ECL; bottom panel: the membrane was stripped and re-probed for total TrxR.

Figure 6. Inhibition of pancreatic xenograft tumor growth in nude mice following treatment with indolequinones. MIA PaCa-2 xenograft tumors were grown on the flanks of nude mice and then treated with selected indolequinones (1.0 and 2.5 mg/kg i.p.) every other day for 20 d. Mice were weighed twice weekly and neither the control mice nor the treatment groups suffered significant weight loss or any apparent toxicity. Tumor volume was calculated by the formula $(L \times W^2)/2$, where L is the longer measurement of the tumor and W is the smaller tumor measurement. Data represents the mean ± SEM of 6 mice. *, tumor volume in the treatment group was statistically different from controls as determined

Molecular Pharmacology Fast Forward. Published on April 13, 2009 as DOI: 10.1124/mol.109.055855
This article has not been copyedited and formatted. The final version may differ from this version.

by the Dunnett's test.

Figure 7. A proposed mechanism for the inhibition of TrxR by indolequinones. (A) Indolequinone activation by two-electron reduction to generate a reactive iminium electrophile. **(B)** Reduction of oxidized TrxR by NADPH to generate the reduced C-terminal selenocysteine. **(C)** Inhibition of TrxR via alkylation of the reduced C-terminal selenocysteine by the reactive indolequinone iminium electrophile.

Molecular Pharmacology Fast Forward. Published on April 13, 2009 as DOI: 10.1124/mol.109.055855
This article has not been copyedited and formatted. The final version may differ from this version.

Table 1: Structure of Indolequinones

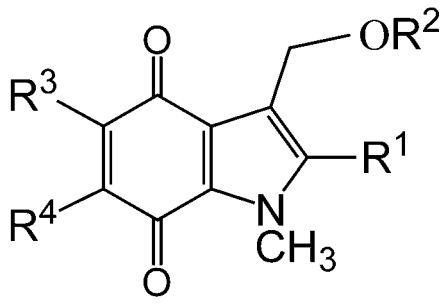

Compound	R^1	R^2	R^3	R^4
1 (ES936)	CH_3	4-NO_2-C_6H_4	OCH_3	H
2	CH_3	4-NO_2-C_6H_4	H	OCH_3
3	CH_2OH	4-NO_2-C_6H_4	OCH_3	H
4	CH_2OH	2,4,6-F_3-C_6H_2	OCH_3	H
5	CH_2OH	4-NO_2-C_6H_4	H	OCH_3
6	H	4-NO_2-C_6H_4	H	OCH_3
7	H	2,4,6-F_3-C_6H_2	H	OCH_3
8	H	4-NO_2-C_6H_4	OCH_3	H
9	H	2,4,6-F_3-C_6H_2	OCH_3	H

Table 2. IC_{50} Values for Indolequinones in Pancreatic Cancer Cell Lines[a].

Compound	IC_{50} (nM)					
	PANC-1		MIA PaCa-2		BxPC-3	
	4 h	72 h	4 h	72 h	4 h	72 h
1 (ES936)	788 ± 51	88 ± 13	629 ± 73	507 ± 35	408 ± 53	305 ± 24
2	476 ± 50	194 ± 26	638 ± 54	354 ± 48	476 ± 40	285 ± 29
3	120 ± 9	88 ± 3	96 ± 11	74 ± 7	163 ± 25	103 ± 12
4	181 ± 12	80 ± 5	87 ± 9	52 ± 5	329 ± 17	179 ± 16
5	110 ± 15	56 ± 8	72 ± 3	59 ± 10	ND[b]	ND[b]
6	49 ± 4	24 ± 3	32 ± 9	18 ± 5	ND[b]	ND[b]
7	242 ± 13	115 ± 11	26 ± 7	19 ± 4	ND[b]	ND[b]
8	89 ± 7	37 ± 5	39 ± 13	24 ± 6	190 ± 8	79 ± 5
9	ND[b]	ND[b]	34 ± 9	18 ± 6	100 ± 11	43 ± 10

[a]Calculated IC_{50} values are the mean ± SD of three independent determinations using the MTT growth inhibition assay.
[b]ND, not determined.

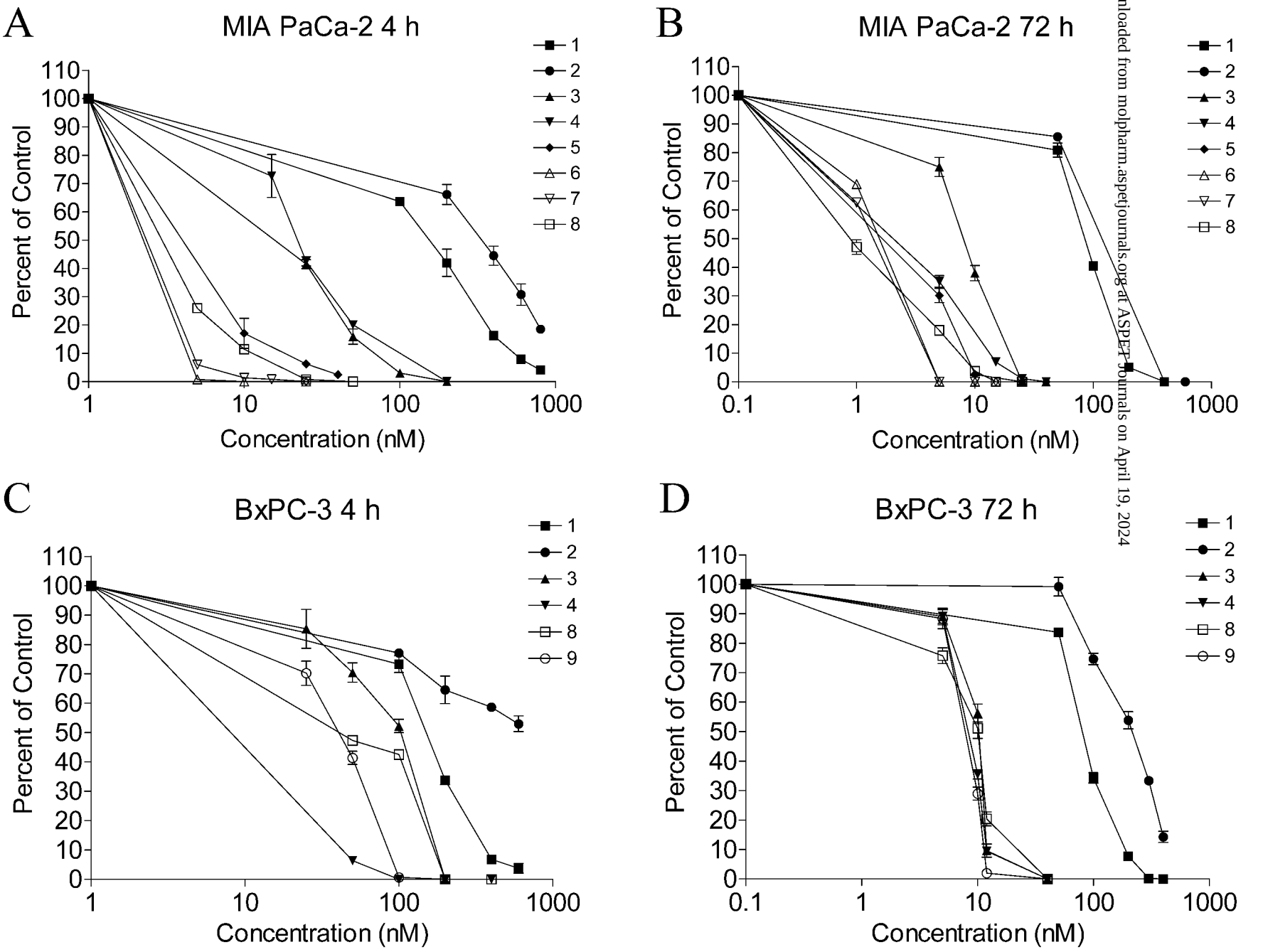

Figure 1

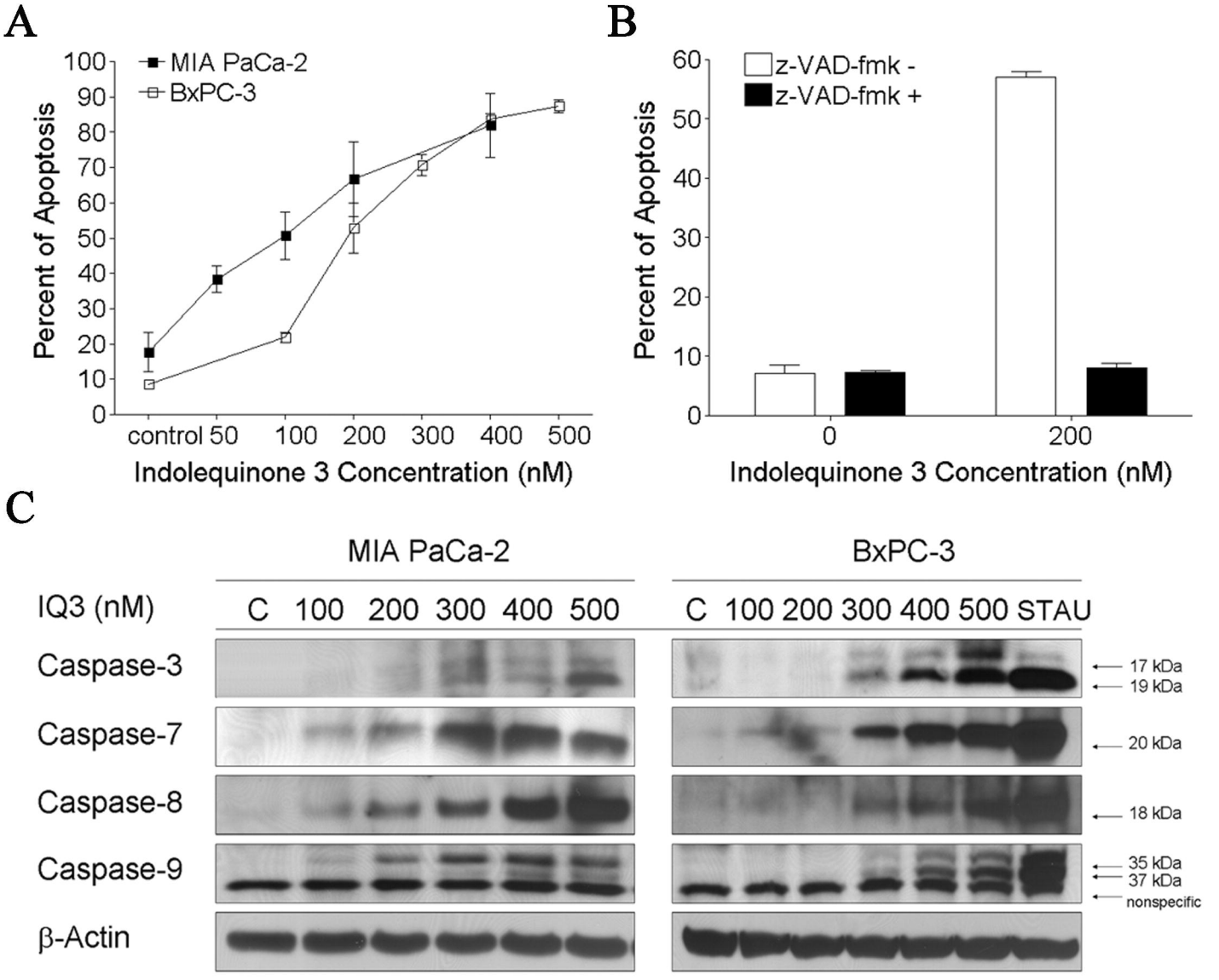
A
MIA PaCa-2
BxPC-3
Percent of Apoptosis
Indolequinone 3 Concentration (nM)
control 50 100 200 300 400 500
B
z-VAD-fmk -
z-VAD-fmk +
Percent of Apoptosis
Indolequinone 3 Concentration (nM)
C
MIA PaCa-2
BxPC-3
IQ3 (nM)
C 100 200 300 400 500
C 100 200 300 400 500 STAU
Caspase-3
Caspase-7
Caspase-8
Caspase-9
β-Actin
17 kDa
19 kDa
20 kDa
18 kDa
35 kDa
37 kDa
nonspecific

Figure 2

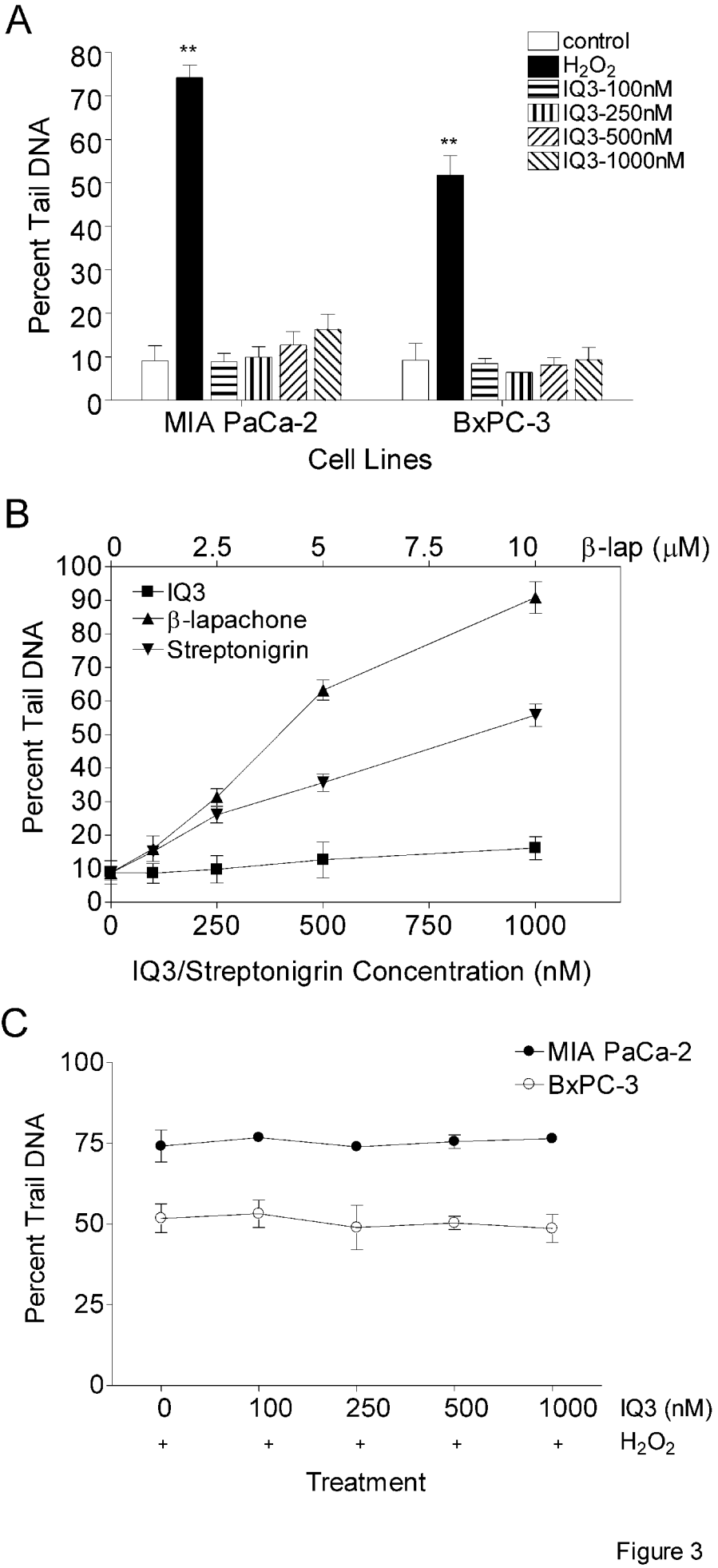
A
control
H2O2
IQ3-100nM
IQ3-250nM
IQ3-500nM
IQ3-1000nM
Percent Tail DNA
MIA PaCa-2
BxPC-3
Cell Lines
B
β-lap (μM)
IQ3
β-lapachone
Streptonigrin
Percent Tail DNA
IQ3/Streptonigrin Concentration (nM)
C
MIA PaCa-2
BxPC-3
Percent Trail DNA
IQ3 (nM)
H2O2
Treatment

Figure 3

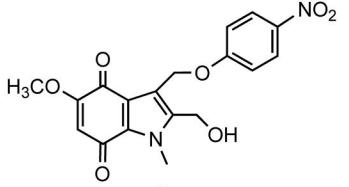

3

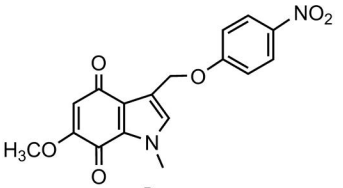

6

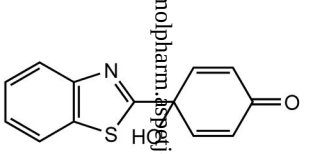

AW464

Panel/Cell Line	Log_{10}LC50	LC50
Leukemia		
CCRF-CEM	> -4.00	
HL-60(TB)	> -4.00	
K-562	> -4.00	
MOLT-4	> -4.00	
RPMI-8226	> -4.00	
SR	> -4.00	
Non-Small Cell Lung Cancer		
A549/ATCC	-5.07	
EKVX	-5.44	
HOP-62	-5.51	
HOP-92	-5.19	
NCI-H226	-5.27	
NCI-H23	-5.14	
NCI-H322M	-5.51	
NCI-H460	-5.08	
NCI-H522	-5.97	
Colon Cancer		
COLO 205	-6.13	
HCC-2998	-6.13	
HCT-116	-4.89	
HCT-15	-5.72	
HT29	-5.34	
KM12	-5.69	
SW-620	-5.60	
CNS Cancer		
SF-268	-5.52	
SF-295	-5.21	
SF-539	-5.46	
SNB-19	-5.37	
SNB-75	-5.43	
U251	-5.53	
Melanoma		
LOX IMVI	-5.00	
MALME-3M	-6.16	
M14	-5.19	
SK-MEL-2		
SK-MEL-28	-5.66	
SK-MEL-5	-5.28	
UACC-257	-5.31	
UACC-62	-5.59	
Ovarian Cancer		
IGROV1	-5.29	
OVCAR-3	-6.26	
OVCAR-4	-5.44	
OVCAR-5	-5.69	
OVCAR-8	-5.30	
SK-OV-3	-5.06	
Renal Cancer		
786-0	-5.47	
A498	-5.39	
ACHN	-5.60	
CAKI-1	-5.78	
RXF 393	-5.33	
SN12C	-5.47	
TK-10	-6.27	
UO-31	-5.50	
Prostate Cancer		
PC-3	> -4.00	
DU-145	-5.70	
Breast Cancer		
MCF7	-5.05	
NCI/ADR-RES	-4.98	
MDA-MB-231/ATCC	-5.49	
HS 578T	-4.60	
MDA-MB-435	-5.69	
BT-549	-5.72	
T-47D	> -4.00	
MDA-MB-468	-4.36	
MID	-5.25	
Delta	1.02	
Range	2.27	

+3 +2 +1 0 -1 -2 -3

Panel/Cell Line	Log_{10}LC50	LC50
Leukemia		
CCRF-CEM	-4.00	
HL-60(TB)	-4.00	
K-562	-4.00	
MOLT-4	-4.00	
RPMI-8226	-4.00	
SR	-4.00	
Non-SmallCellLung		
A549/ATCC	-4.16	
EKVX	-4.62	
HOP-62	-5.23	
HOP-92	-5.04	
NCI-H226	-5.28	
NCI-H23	-4.91	
NCI-H322M	-4.20	
NCI-H460	-5.31	
NCI-H522	-5.28	
Colon		
COLO205	-5.83	
HCC-2998	-6.38	
HCT-116	-5.74	
HCT-15	-5.64	
HT29	-5.09	
KM12	-6.09	
SW-620	-6.28	
CNS		
SF-268	-5.38	
SF-295	-4.00	
SF-539	-5.80	
SNB-19	-4.00	
SNB-75	-5.16	
U251	-5.53	
Melanoma		
LOXIMVI	-5.51	
MALME-3M	-6.07	
M14	-5.13	
SK-MEL-2	-5.83	
SK-MEL-28	-6.19	
SK-MEL-5	-4.96	
UACC-257	-5.42	
UACC-62	-5.80	
Ovarian		
IGROV1	-5.55	
OVCAR-3	-5.84	
OVCAR-4	-5.38	
OVCAR-5	-5.59	
OVCAR-8	-5.14	
SK-OV-3	-4.48	
Renal		
786-0	-5.73	
A498	-4.90	
ACHN	-5.64	
CAKI-1	-5.60	
RXF393	-5.98	
SN12C	-5.71	
TK-10	-5.67	
UO-31	-5.46	
Prostate		
PC-3	-4.17	
DU-145	-5.49	
Breast		
MDA-MB-435	-6.23	
NCI/ADR-RES	-4.00	
MCF7	-4.60	
MDA-MB-231/ATCC	-5.36	
HS578T	-4.00	
BT-549	-5.13	
T-47D	-4.00	
summary		
MG_MID	-5.14	
Delta	1.14	
Range	2.38	

3 2 1 0 -1 -2 -3

Panel/Cell Line	Log_{10}LC50	LC50
Leukemia		
CCRF-CEM	-5.59	
HL-60(TB)	-6.13	
K-562	> -4.00	
MOLT-4	> -4.00	
RPMI-8226		
SR	> -4.00	
Non-Small Cell Lung Cancer		
A549/ATCC	-4.36	
EKVX	-5.24	
HOP-62	-4.90	
HOP-92	-5.43	
NCI-H226	-4.63	
NCI-H23	-5.29	
NCI-H322M	-4.63	
NCI-H460	-4.35	
NCI-H522		
Colon Cancer		
COLO 205	-5.29	
HCC-2998	-6.01	
HCT-116	-6.33	
HCT-15	-5.61	
HT29	-6.16	
KM12	-5.36	
SW-620	> -4.00	
CNS Cancer		
SF-268	-5.20	
SF-295	-5.33	
SNB-75	-5.33	
U251	-5.59	
Melanoma		
LOX IMVI	-5.42	
MALME-3M	-5.63	
M14	-5.28	
SK-MEL-2	-5.15	
SK-MEL-28	-5.60	
SK-MEL-5	-4.62	
UACC-257	-5.01	
UACC-62	-5.24	
Ovarian Cancer		
IGROV1	-5.27	
OVCAR-3	-5.54	
OVCAR-4	-5.42	
OVCAR-5	-5.73	
OVCAR-8	-5.30	
SK-OV-3	-4.42	
Renal Cancer		
786-0	-5.98	
A498	-5.07	
ACHN	-5.56	
CAKI-1	-5.87	
RXF 393	-6.24	
SN12C	-5.84	
UO-31	-6.02	
Prostate Cancer		
DU-145	-5.47	
Breast Cancer		
MCF7	-5.39	
NCI/ADR-RES	> -4.00	
MDA-MB-231/ATCC	-5.24	
HS 578T	> -4.00	
MDA-MB-435	-5.82	
MDA-N	-6.00	
BT-549	-5.32	
T-47D		
MG_MID	-5.25	
Delta	1.08	
Range	2.33	

+3 +2 +1 0 -1 -2 -3

Colon

Melanoma

Renal

Figure 4

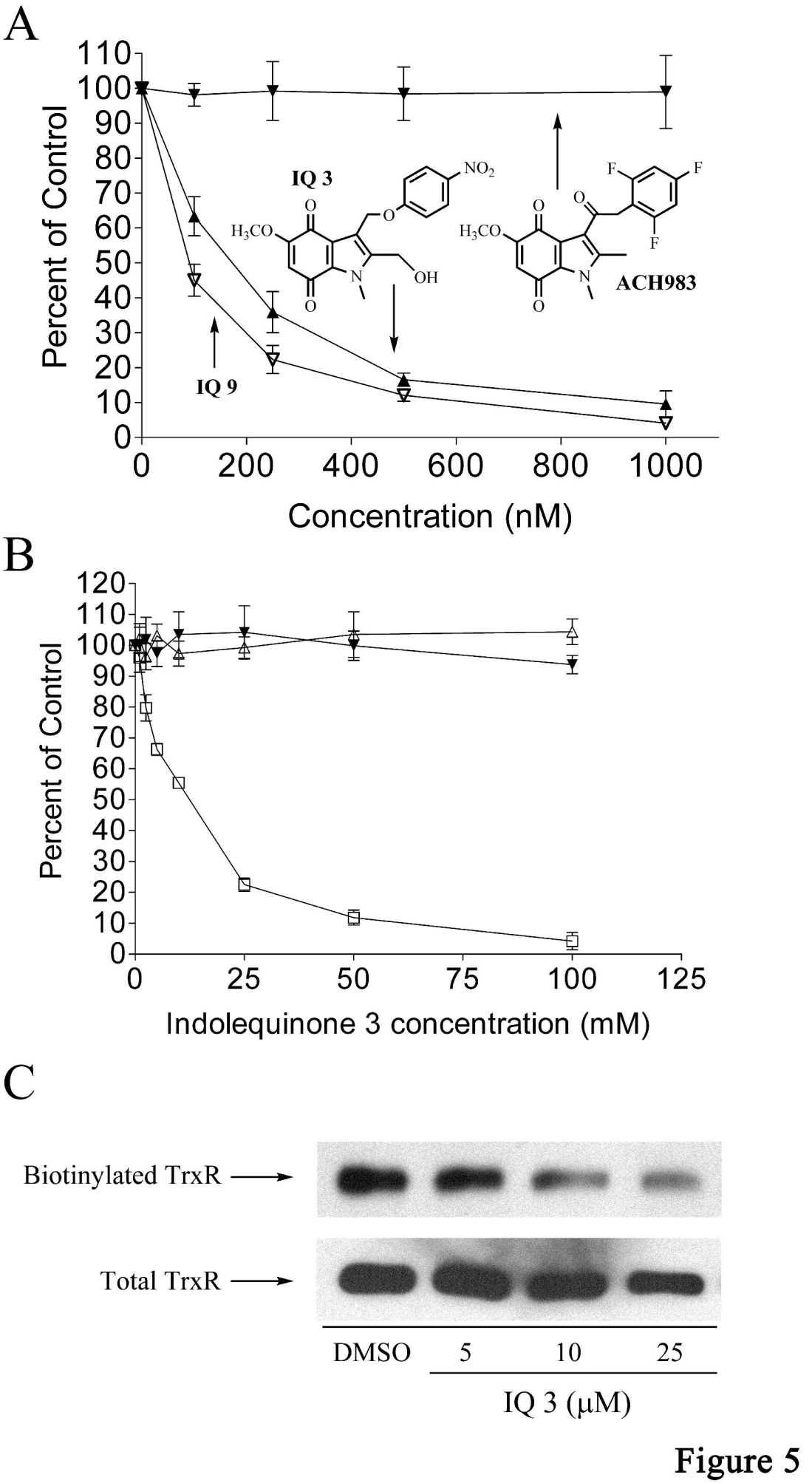
A
Percent of Control
Concentration (nM)
IQ 3
ACH983
IQ 9
B
Percent of Control
Indolequinone 3 concentration (mM)
C
Biotinylated TrxR
Total TrxR
DMSO
5
10
25
IQ 3 (μM)

Figure 5

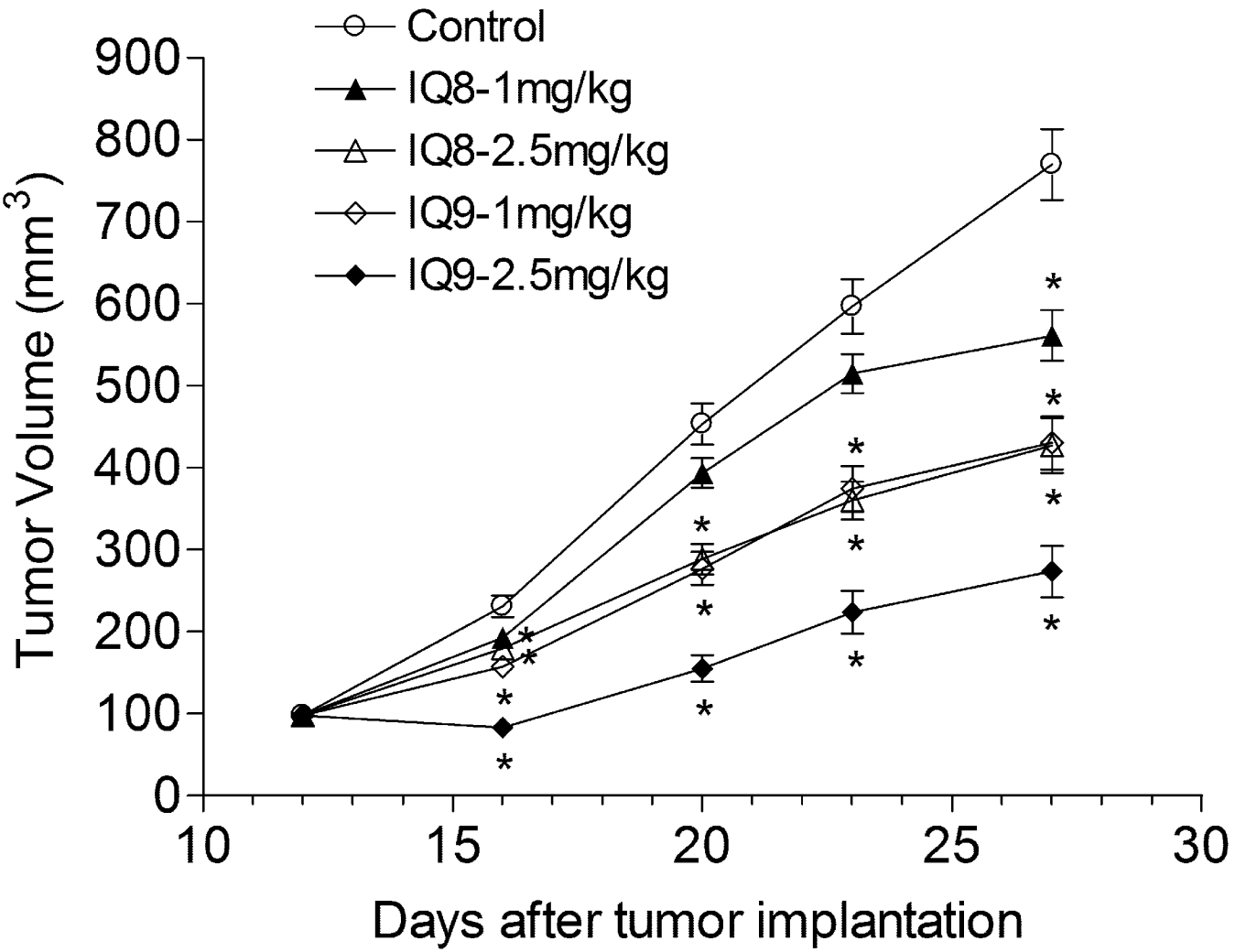
Control
IQ8-1mg/kg
IQ8-2.5mg/kg
IQ9-1mg/kg
IQ9-2.5mg/kg
Tumor Volume (mm3)
900
800
700
600
500
400
300
200
100
0
10
15
20
25
30
Days after tumor implantation

Figure 6

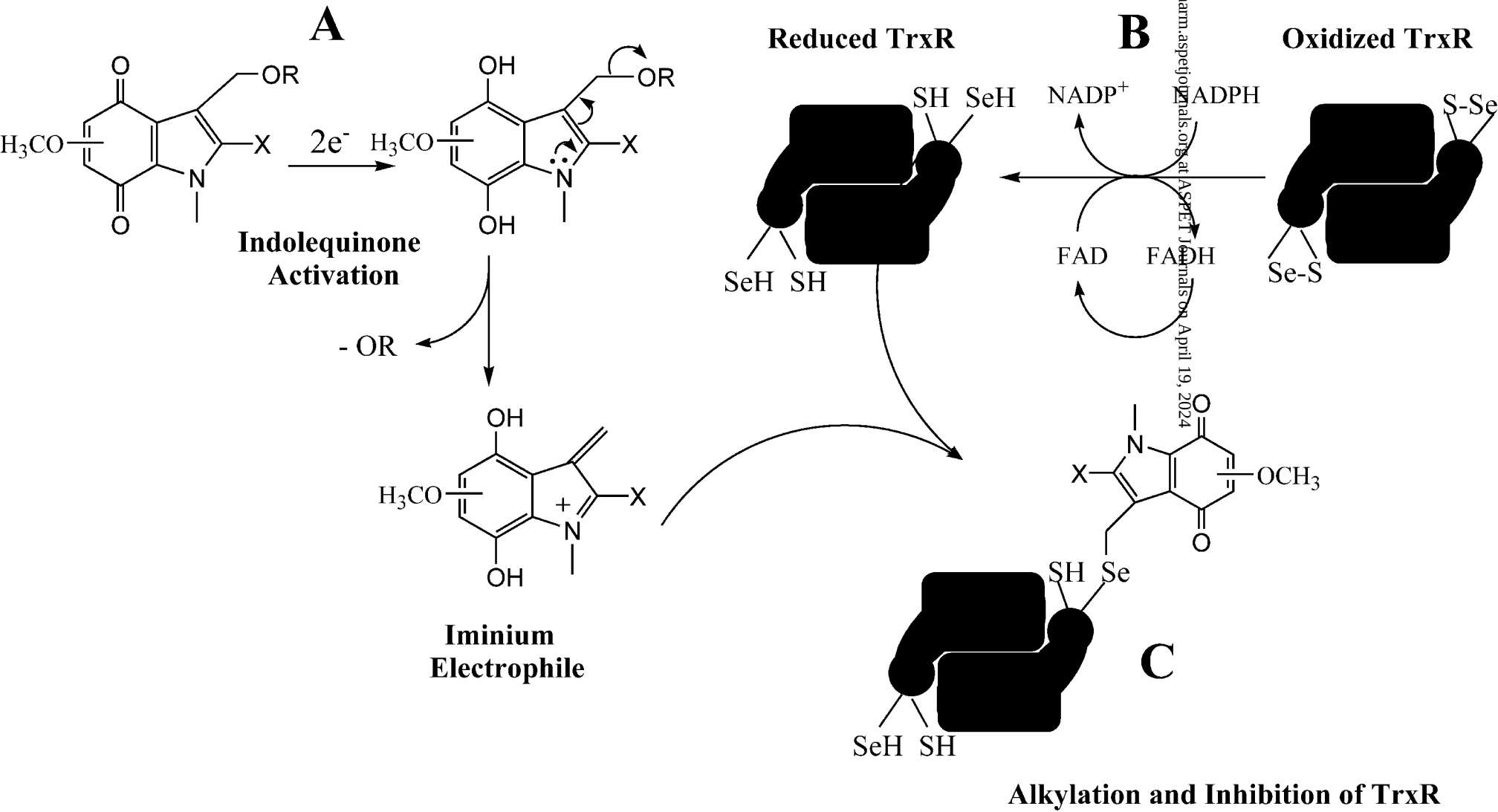

Figure 7